



Enhancement of mechanical and physical properties of electrospun PAN nanofiber membranes using PVDF particles

Raed M. Elkhaldi^{a,b,c}, Serkan Guclu^{a,b}, Ismail Koyuncu^{a,b,*}

^aNational Research Center on Membrane Technologies, Istanbul Technical University, Maslak, 34469 Istanbul, Turkey, emails: raedmkhaldi@hotmail.com (R. Alkhaldi), gucluse@hotmail.com (S. Guclu), koyuncu@itu.edu.tr (I. Koyuncu)

^bDepartment of Environmental Engineering, Istanbul Technical University, Maslak, 34469 Istanbul, Turkey

^cEnvironmental and Earth Sciences Department, Islamic University of Gaza, Gaza, Gaza Strip 108, Palestine

Received 3 November 2015; Accepted 18 February 2016

ABSTRACT

In this study, polyacrylonitrile (PAN) nanofiber mats were fabricated using electrospinning method. Three hundred nanometers of polyvinylidene fluoride (PVDF) fine particles were used to enhance the mechanical strength and structural integrity of the as-spun nanofibrous membrane. As-spun nanofibrous mats were submerged in different concentrations of PVDF dispersions to incorporate PVDF particles among PAN nanofibers matrix. Subsequently, they were subjected to post-heat treatment at 177°C. The fused PVDF cemented the strings and welded the junctions that resulted in strengthening the fibers and enhancing its bonding together. The PVDF-cemented PAN (PVDF-c-PAN) membranes were characterized by scanning electron microscopy, dynamic mechanical analysis, porometry, and permeability analysis. Results showed good improvement in the membranes' mechanical properties in terms of tensile strength and Young's modulus. Comparing to as-spun PAN, the average increase in Young's modulus and tensile strength in the PVDF-c-PAN membranes were 19.8 and 6.63 folds, respectively. However, the strain ratio decreased by 5.47 folds. The highest improvement was obtained by PVDF-c-PAN membrane at 0.01 wt.% PVDF and one second submersion time. In comparison with two different techniques that seek the same purpose, this technique is simpler, applicable, and time–cost saving.

Keywords: PAN; PVDF; Mechanical properties; Electrospinning; Nanofiber

1. Introduction

Electrospinning is a novel, versatile, and affordable technique to produce nanofiber membranes from polymer solutions or melts [1,2]. Nanofibers are generally employed for a wide scope of uses, such as air filters [3], membrane separation [4], catalysts [5], conductive fiber [6], energy scavenging [7], ultrasensitive sensors

[8], micro/nanoactuators [9], tissue engineering scaffolds [10], drug delivery [11], protective clothing [12], and multifunctional composites [13]. Most of these applications require certain mechanical properties and robustness [14].

Electrospun nanofibrous membranes (ENMs) are relatively newly developed materials in the filtration field. Widespread commercialization of these materials has been impeded by poor mechanical stability, which mostly refers to their high porosity exacerbated with

*Corresponding author.

weak bonding at fiber junctions [15]. The choice of a polymer for a specific application should be based on a key criterion for that application and should also be based on cost. In some applications, such as FO–MBR, membrane tensile strength and tolerance against applying stresses is very important to resist the mechanical deformation caused by a broad range of temperature, humidity, mechanical vibration, shock, reactive, and abrasive particulates, while for instance, in sea water desalination using forward osmosis technology, high flux may be a critical need and may override other features such as mechanical resistance as there is no or little pressure used.

Polyacrylonitrile (PAN) is a synthetic, semi-crystalline organic polymer resin that widely used for electrospun nanofiber membrane fabrication due to chemical stability, solubility in common solvents, hydrophilicity, and low fouling propensity [16]. Nevertheless, PAN membranes show mechanical shortcomings related to brittleness and pore collapse, especially when it exposed for sequential rounds of wet and dry conditions [17]. PAN has a special mode as it degrades before melting at 317°C if the heating rates are 50 degrees per minute or above [18,19]. Jiang et al. [20] investigated the structural change of PAN fibers and their results showed that above 87°C (its glass transition temperature) and below 180°C minimal structural change was detected. While from 180 to 240°C, partial thermal degradation was noticed without change of its original backbone structure. Polyvinylidene fluoride (PVDF) is characterized by its toughness, strength, non-reactivity, and tolerance to extreme thermal and chemical conditions. Furthermore, its relatively low melting point (177°C) and easy melting process can provide it with eligibility to play a role of cement material to strengthen the fiber junctions in electrospun fiber mat [21].

The mechanical characteristics of electrospun nanofiber rely mainly on the polymer composition, in addition to fiber orientation, arrangement, size, and molecular structure.

During its service lifetime in different real-life applications, the nanofibers could be exposed to mechanical stresses leading to permanent deformation or even failure [22]. Therefore, commercially based produced membrane should have high mechanical strengths and superior stiffness, in addition to anti-fouling, chemical resistance, thermal stability, high selectivity, and good flux.

Wang et al. [23] classified the previous studies that targeted the enhancement of mechanical strength of ENMs into three categories. In some researches, non-woven fibers redesigned to be changed from conventional web structure to self-bundled fiber strings.

Adding nanoadditives into the polymer solution to incorporate and reinforce the electrospun fiber matrix is the second approach to promote the mechanical properties. However, these nanoadditives are normally difficult to fabricate, not easy to evenly disperse and costly.

Probably post-heat treatment by exposing as spun mat to heating above its glass transition temperature but below melting point, considers the most effective approaches to enhance the bonding at junction points by soldering the fibers together [15].

Bilad et al. [24] investigated the feasibility of using nanofiber membranes as potential MBR-membranes. In this study, the impact of post-heat treatment on nanofiber membrane was studied and showed remarkable improvement of membrane performance against layered fouling, but also demonstrated a lowering of critical flux. Exposing electrospun fibers to a temperature near below their melting points, the enhanced stability of fibers by changing their crystallinity and facilitated the linking of melted nanofibers to one another.

Homaeigohar and Elbahri [25] reinforced PES electrospun nanofiber membrane against compaction via adding Zirconia nanoparticles into nanofiber matrix which resulted in improving mechanical strength and wettability. Yoon et al. [26] enhanced mechanical properties using two different solvents, DMF and NMP in electrospinning solution. Less volatile NMP is a high boiling solvent and can leave nanofiber matrix more slowly, leading to fusion of nanofiber junction points. Using NMP with DMF (50%: 50%), mechanical strength and Young's modulus were improved by 570 and 360% respectively. Zhang et al. [27] electrospun polymer blends, PAN and PA-66 simultaneously. They used PA-66 nanofibers between PAN nanofibers to improve mechanical properties of their membrane.

Apart from being used in filtration applications, void-free electrospun non-woven PA6 nanofibers were produced using a solution-based processing method to optimize the membranes mechanical properties. PA6 electrospun fiber mats were introduced into PVA solution. After the evaporation of the solvent, the PVA matrix filled all the pores [28]. A recent study investigated the potential use of polyphenylsulfone (PPSU) nanofibrous membrane in the filtration of canned beans production wastewater. A heat-treated PPSU nanofibrous membrane with a mean fiber diameter of 694 nm showed 100% turbidity rejection, while obtaining chemical oxygen demand and total dissolved solid rejections of 27 and 25%, respectively [29].

Although a combination of high strength and toughness is the crucial necessity and the most challenging for all structural materials research,

unfortunately, most of the studies attain success in terms of mechanical strength enhancement were partially at the expense of strain and toughness [30,31]. For example, metals and polymers that are drawn to high draw ratios exhibit remarkable strength and modulus but low failure strains.

Since developed in the 1960s, high-performance fibers used as the reinforcement phase are considered a milestone of structural materials industrialization, due to its very high strength, heat resistance, and chemical stability. Nevertheless, most of the current fibers are brittle and the majority of the structural fibers break at low strains [32]. Papkov et al. [33] succeeded to synchronously improve elastic modulus from 0.36 to 48 GPa, true strength from 15 to 1,750 MPa, and toughness from 0.25 to 605 MPa when reduced the fiber diameter up to 100 nm. The increase of toughness attributed to low nanofiber crystallinity at that diameter ranges.

Conversely, for the integration of nanocomposite material in the electrospun polymer solution, the as-spun PAN-based nanofiber mats were introduced to PVDF-contained solution and post-heat treated at 177°C afterward. The melted PVDF particles played the role of cement for the fiber strings and fused them together at junction points. This is expected to lead to the improvement of its mechanical properties.

Obtaining the optimum membrane production conditions was targeted as one of the technical objectives of this work. Effects of PVDF concentration and submersion time on the membrane were studied. Our results revealed that membrane A that submerged in 0.01 wt.% PVDF for one second had almost the best mechanical strength and relatively the lowest permeability reduction.

2. Material and methods

2.1. Material

The PAN polymer (Mw: 150000 Da) and surfactant Triton X-100 used in this study were obtained from Sigma-Aldrich. DMF was purchased from Akkim (Turkey) and used as a solvent without any further purification. KYNAR 500, fine powder-grade PVDF polymer with 300 nm diameter was purchased from Arkema.

2.2. Nanofiber membrane production

About 8% w/w PAN solution was prepared using DMF as a solvent. The solution stirred on a magnetic stirrer plate for a period of 24–36 h at 310 rpm and 30°C until the solution became homogeneous.

Nanofiber membranes were fabricated using electrospinning machine (NE100, Inovenso Co. Ltd, Turkey). It has a grounded collection drum which rotates constantly at 350 rpm and strokes to both sides in order to collect nanofibers uniformly. Each polymer solution was electrospun through four metallic nozzles, each having 700 µm inner diameters. Production of electrospun PAN-based membrane was performed at room temperature for two hours. For all the membranes fabrication, the flow rate of 4 mL/h, voltages of 27 kV, and nozzle tips to collector drum distance of 13 cm were selected as electrospinning operating parameters.

2.3. Using PVDF particles for PAN mat cementation

Different concentrations of a fine powder grade, KYNAR 500 PVDF (Arkema) dispersions were prepared. Average diameter of PVDF nanoparticles was about 300 nm. For each concentration, the specific amount of PVDF is added to 400 ml of distilled water containing 4 g of Triton X-100 (Sigma-Aldrich). Magnetic stirrer and ultra-sonication bath were used to disperse PVDF particles. Dispersions were ultra-sonicated for at least 2 h before the experiments.

25 × 15 cm pieces of the electrospun PAN membranes were submerged in different PVDF dispersion concentrations for different submersion periods. The concentrations and submersion times for the PVDF-c-PAN membranes are shown in Table 1.

PAN membrane pieces containing PVDF particles were transferred into 177°C oven and dried for 10 min to allow the melting of PVDF among electrospun PAN fibers. Different PVDF-c-PAN with different concentrations and submersion times are referred to as A, B, C, and D, while as-spun PAN is labeled as blank-control. Steps of PVDF-c-PAN membrane synthesis are illustrated in Fig. 1.

2.4. Characterization

In order to determine the effect of PVDF addition on the PAN membrane and its characteristics, four tests were performed which included permeability, scanning electron microscopy (SEM), dynamic mechanical analysis (DMA), and porometry.

2.4.1. Filtration test (water flux measurements on as-spun PAN and PAN-c-PVDF membranes)

The permeability of the membranes was determined by water flux measurements. The pure water flux was characterized in dead-end filtration cells (Sterlitech Corp., Kent, USA). Approximately 1,000 mL

Table 1
PVDF concentrations and submersion times for as-spun PAN and PVDF-c-PAN membranes

Serial no.	Membrane	PVDF conc. (wt.%)	Submersion time	Symbol
1	PVDF-c-PAN	0.01	1 s	A
2	PVDF-c-PAN	0.01	10 s	B
3	PVDF-c-PAN	0.05	1 s	C
4	PVDF-c-PAN	0.05	10 s	D
5	As-spun PAN	–	–	Blank

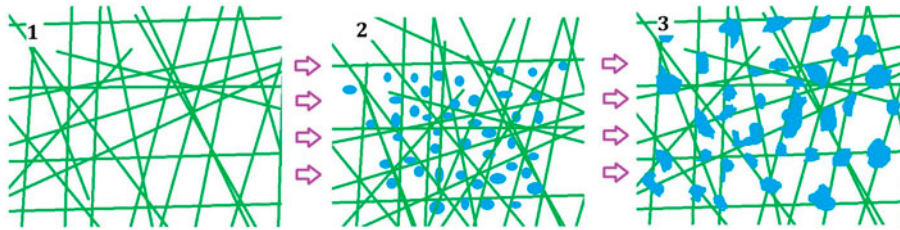


Fig. 1. Steps of PVDF-c-PAN membrane synthesis.

Notes: (1) PAN nanofiber, (2) incorporation of PVDF particles on/into PAN nanofibers, (3) melting of PVDF to cement PAN nanofibers.

of ultrapure water was allowed to permeate through the membranes at 0.6 bars for compaction. For each membrane, water flux experiments were performed at 0.2, 0.4, and 0.6 bars and calculated using the following equation:

$$J = \frac{V}{A\Delta t} \quad (1)$$

where V is the permeate volume (L), A is the effective membrane area (m^2), and Δt is the filtration time (h). Using Microsoft Excel, flux vs. pressure was plotted. From the slope of the graph, permeability results were obtained.

2.4.2. Scanning electron microscopy

The microstructure of the PVDF-c-PAN nanofiber mats were observed with an FEI Quanta FEG 250 scanning electron microscope (SEM) after being coated with Au–Pd by using Quorum SC7620 ion sputtering.

2.4.3. Dynamic mechanical analysis

The tensile strength, strain, and Young's modulus of PVDF-c-PAN nanofiber mat according to ASTM D638 were measured by SII DMS 6100 Exstar. The machine was operated under a displacement control mode at the crosshead speed of 5 mm/min.

2.4.4. Porometer test

Pore size and pore size distribution of the nanofibrous membranes have been studied using a capillary flow porometry. Quantachrome's Porofil with a defined very low surface tension of 16 dynes/cm (Quantachrome Ins., Florida, USA) was used as a wetting agent for porometry measurements. Membranes were cut into 3×3 cm squares for porometry measurements. The thickness of the prepared samples was measured electronically using the micrometer.

3. Results and discussion

3.1. Preliminary experiments

Early in this work, different PAN concentrations with different electrospinning operating conditions were tested to optimize the dope solution and the fabrication process criteria. The characterization of this stage restricted to SEM micrographs that can be evaluated the fiber structure (beadless, fiber radius) through. For example, 6 wt.% PAN solution was used to fabricate nanofibrous web. Unfortunately, bead-on-string structure was observed as seen in Fig. 2. Research team considered two conditional boundaries in the fabrication process. Firstly, the smaller the fiber radius, the greater is the mechanical stability. Moreover, the smaller is the developed pore size, which result in better filterability. The second boundary is

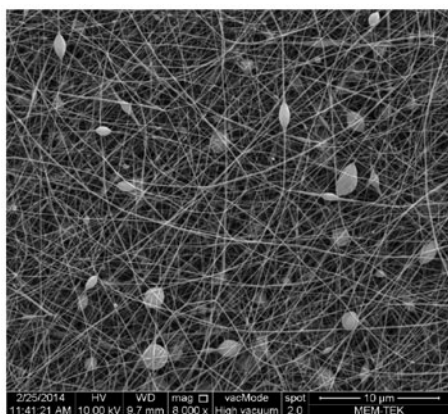


Fig. 2. A SEM micrographs of nanofibrous membranes doped from 6 wt.% PAN solution at 8,000 magnifications.

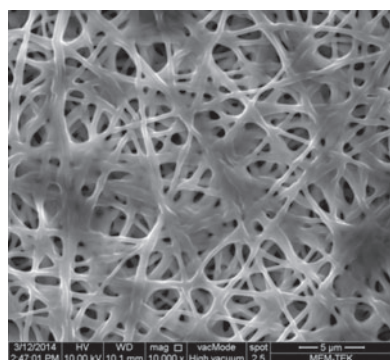
the production of uniform beadless fibers as the beads-on-strings structure is a mechanical shortcoming sign. The amount of beads increased with decreased

polymer concentration because the very low viscosity did not suffice to sustain the elongation of the liquid jet. But, the fiber radius also increased with the increase of polymer concentration [34].

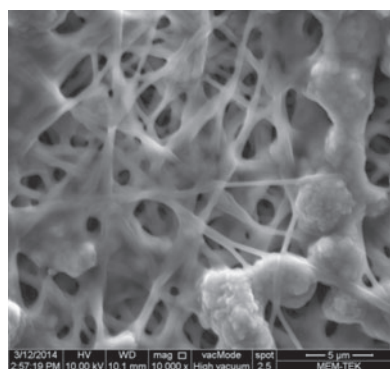
Process parameters were optimal for 8 wt.% PAN polymer spun at a flow rate of 4 mL/h, with a tip to a collector distance of 13 cm, and an applied voltage of 27 kV. Later, numbers of these membranes were synthesized for further PVDF treatment. For more homogeneity and eventual distribution of PVDF upon the surface and through the fiber matrix, nonionic surfactant (Triton X-100) was used. Determination of the lowest PVDF concentration that can enhance the mechanical stability without sacrificing the membrane permeability was also investigated.

Number of PAN membranes were submerged in 0.1, 0.5, 1.0, and 2.0 wt.% PVDF solutions for one second and then further post-heat treated. The SEM micrographs of these membranes at 10,000 magnifications are presented in Fig. 3.

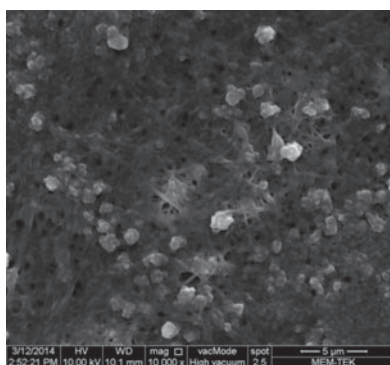
The SEM micrographs showed high agglomeration of PVDF particulates on the surfaces of the



0.1 wt.% PVDF-c-PAN membrane



0.5 wt.% PVDF-c-PAN membrane



1.0 wt.% PVDF-c-PAN membrane



2.0 wt.% PVDF-c-PAN membrane

Fig. 3. A series of SEM micrographs for 0.1, 0.5, 1.0, and 2.0 wt.% PVDF-c-PAN membranes at 10,000 magnifications.

membranes. This agglomeration was more pronounced at the higher concentrations such as 1.0 and 2.0 wt.% PVDF-c-PAN. The PVDF particulates could not completely and evenly embed into the nanofiber matrix and the handled fibers membrane surface became rougher at that high concentrations. Because the agglomeration could be considered a negative sign, high PVDF concentrations were excluded and finer concentration range was selected for the next investigation.

3.2. Effect of PVDF concentration and submersion time on the membrane morphology

Based on the preliminary work, finer range of PVDF concentrations at different submersion times were selected for investigation in this stage. The SEM images of the as-spun pure PAN and PVDF-c-PAN nanofiber mats prepared with various PVDF concentrations are presented in Fig. 4. These data indicate that a non-woven mat was created, PVDF has successfully incorporated through the PAN nanofiber matrix, and a fusion of overlapping fibers was noticed.

The SEM images show that membrane A, that was produced at the lowest PVDF concentration and submersion time, had relatively the same morphology when compared to as-spun PAN membrane. The addition of PVDF significantly influenced the fibers diameter and surface. Mean fiber diameter thicknesses

given in Table 2 were calculated from the measurements of fiber diameters in the SEM micrograph.

In membrane A, the addition of 0.01 wt.% PVDF for one second increased the mean fiber diameter by 45%. The largest mean fiber diameter was in membrane D. The higher the concentration of submersion solution, the larger became the fiber thickness. Even though membrane B has the same concentration of membrane A, the increase of contact time has remarkably increased the mean fiber diameter. Regarding membrane B and C, even though the membrane C has been immersed in 0.05 wt.% PVDF solution rather than 0.01 wt.% PVDF solution (membrane B), the mean fiber diameter was higher in the latter inferring that the submersion time is more crucial in building up cement material upon the membrane mate. Cross-section images of the membranes shown in Fig. 5.

Table 2
Mean fiber diameters and Membrane thicknesses

Membrane	Mean fiber diameter (nm)	Membrane thickness (μm)
Blank	294	56.25
A	427	34.04
B	547	35.32
C	536	30.41
D	652	29.7

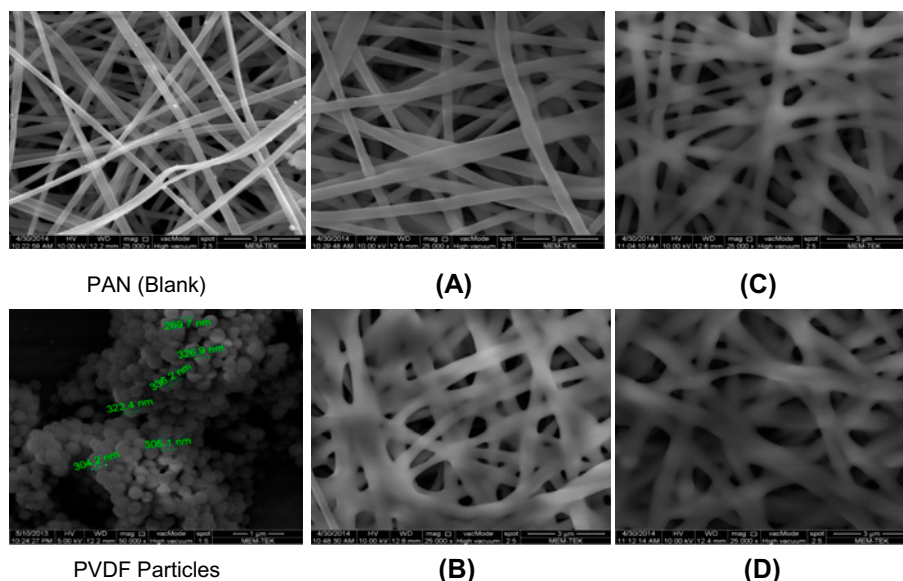


Fig. 4. A series of SEM micrographs for all PVDF-c-PAN membranes at 25,000 \times magnification and for PVDF particles at 50,000 \times magnifications: (A) 0.01 wt.% 1 s, (B) 0.01 wt.% 10 s, (C) 0.05 wt.% 1 s, and (D) 0.05 wt.% 10 s.

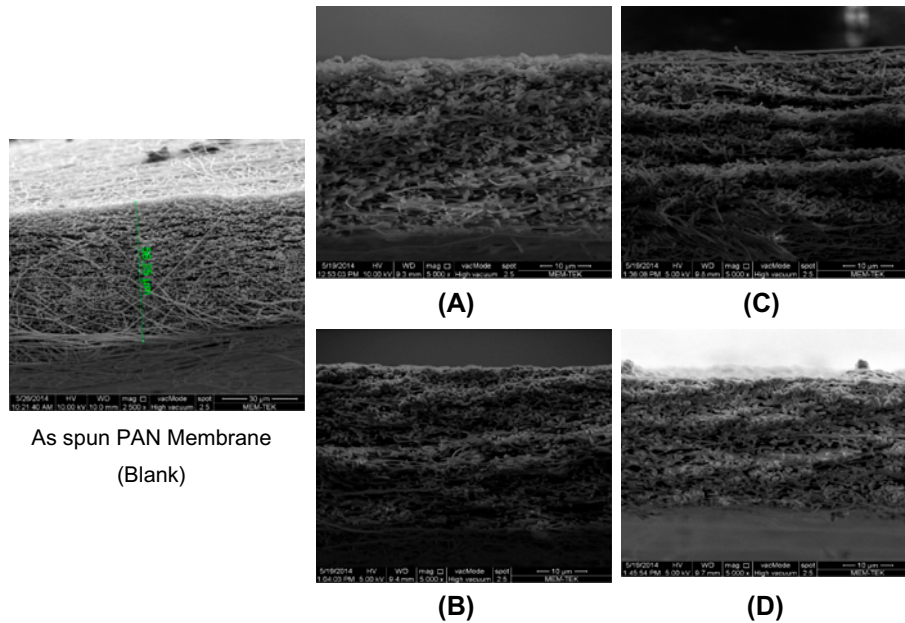


Fig. 5. Cross-section SEM images of as-spun PAN and PVDF-c-PAN nanofibers: (A) 0.01 wt.% 1 s, (B) 0.01 wt.% 10 s, (C) 0.05 wt.% 1 s, and (D) 0.05 wt.% 10 s.

It is noticeable that the melting of PVDF through the PAN membrane matrix decreases the membrane thickness as the concentration and submersion time increases (Table 2). The results showed that as-spun PAN membrane has a thickness of 56.25 μm ; and the PVDF-c-PAN membranes had thicknesses ranging from 29.7 to 35.32 μm .

3.3. Mechanical properties

Mechanical properties represented by strain, tensile strength, and Young’s modulus were determined. The high strain percent of the blank sample and low values of its tensile strength and Young’s modulus reflected the high ductility of the as-spun PAN fiber.

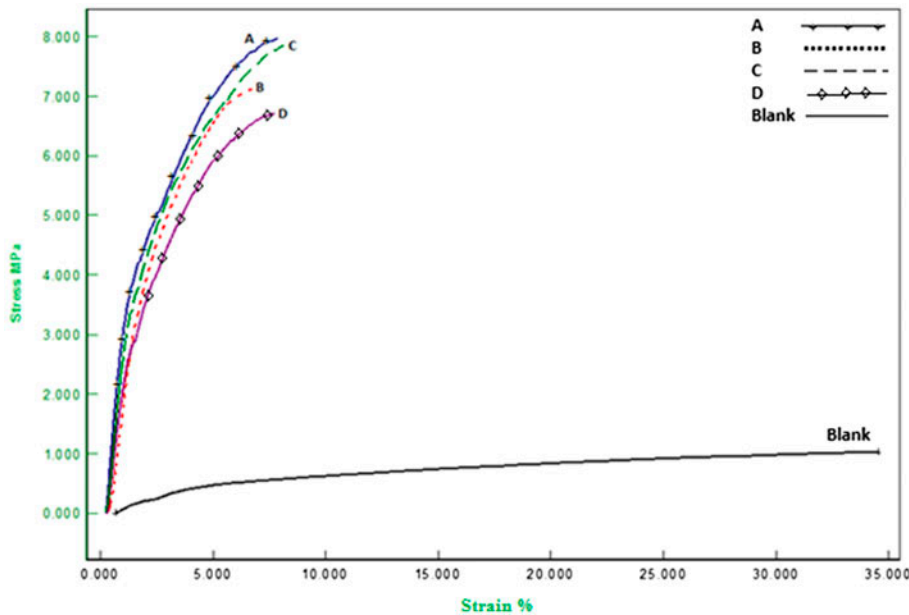


Fig. 6. Stress–strain curves for as-spun PAN and PVDF-C-PAN Nanofibers: (A) 0.01 wt.% PVDF 1 s, (B) 0.01 wt.% PVDF 10 s, (C) 0.05 wt.% PVDF 1 s, (D) 0.05 wt.% PVDF 10 s.

Table 3
Membrane's mechanical property parameters

Sample no.	Young's modulus (MPa)	Tensile strength (Breaking point) (MPa)	Strain (%)
Blank	5.98	1.022	33.86
A	126	7.081	6.231
B	125	5.679	6.00
C	117	6.678	7.254
D	106	7.678	7.794

Fig. 6 illustrates the stress–strain curves for PAN and PVDF-c-PAN nanofibers.

It was shown that the addition of a small amount of PVDF significantly improved tensile strength and Young's modulus, while decreasing the nanofibers strain. The results of membrane mechanical property parameters are shown in Table 3.

Generally, regarding the mechanical properties, no significant differences among the different PVDF-c-PAN membranes were detected. Comparing to blank

sample, the average increase of Young's modulus and tensile strength in the PVDF-c-PAN membranes were 19.8 and 6.63-fold, respectively. However, strain ratio decreased by 5.47-fold.

Data in Table 3 show that membrane A has the best mechanical structure in term of Young's modulus and tensile strength. The water flux measurement values that will be displayed later will reveal that membrane A not only enjoy by better mechanical properties, but also without greatly compromising the membrane flux performance.

The toughness represents the area under the stress–strain diagram. When the increase of the stress is more than the decrease of the strain, it can be concluded there is an overall increase of membrane toughness.

Current research results were compared to two different studies as shown in Table 4. The method described here is quicker, simpler, and cheaper. Comparing to Huang et. al. [15], the post-treatment took shorter time and the mechanical properties were comparable, especially when we take into account the thicknesses of membranes. The composite electrospun

Table 4
Comparative performance among current work, Huang et al. [15], and Hou et al. [35] methods

Author	Current work			Huang et al. [15]			Hou et al. [35]		
Method	Melting post-treatment			Solvent vapor post-treatment			Reinforcing CNTs + hot-stretched post-treatment		
Electrospinning conditions	8% PAN, 27 kV, 4 mL/h, 13 cm			10% PAN, 28 kV, 1 ml/h, 70 rpm			12 wt.%, 14–16 kV, 6.6 m/s		
Post-treatment technique and material	0.01% PVDF was incorporated into PAN mat and melted at 177°C for 10 min			Electrospun nanofibrous membranes (ENMs) were exposed to DMF vapor for 18 h			PAN/SWNTs nanofiber composites were prepared and hot-stretched by fixing one end to the ceiling of the oven and the other end was weighted by 75 g of metal poise to in the temperature-controlled oven at about 135°C for 5 min		
Membrane thickness (µm)	34.04			50–100			–		
	Untreated PAN fiber	Treated PAN fibers	Change (%)	Untreated PAN fibers	Treated PAN fibers	Change (%)	As spun	Hot-stretched	Change (%)
Mechanical properties:									
Tensile strength (MPa)	1.022	7.081	+592	6.5	20	+207	51.84	80.52	+55.32
Young's modulus (MPa)	5.98	126	+2,000	60	500	+733	1,080	2,770	+156
Strain %	33.86	6.231	–443	60	82	+36	22.05	11.61	–90

Table 5
Different membrane porometry data

Sample no.	Blank	A	B	C	D
Pore diameter (μm), at 50% cumulative pore number	≥ 1.36	≥ 0.794	≥ 0.738	≥ 0.745	≥ 0.74
Mean flow pore size (μm)	1.511	0.704	–	–	0.795
Bubble point pressure (bar)	0.315	0.760	0.493	0.622	0.607
Bubble point flow rate (l/m)	0.026	0.071	0.084	0.054	–

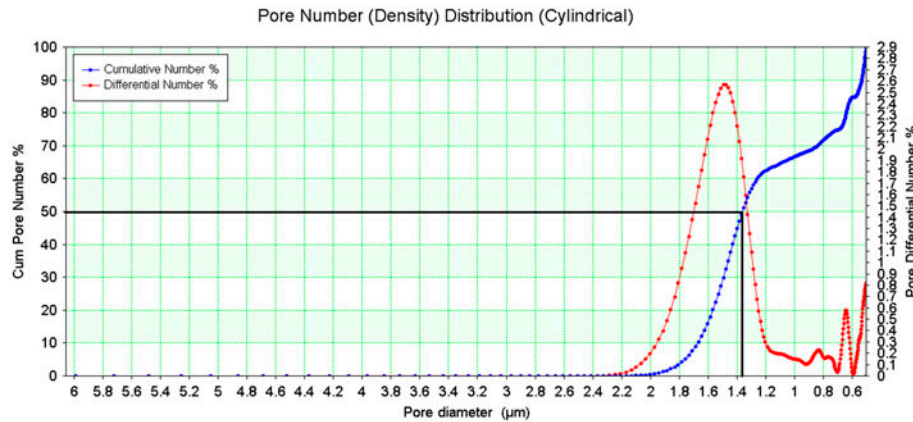


Fig. 7. Pore diameter (μm), at 50% cumulative pore number of the blank sample.

nanofibers show enhanced Young's modulus. However, synthesizing these nanocomposite nanofibers is complicated and costly [35].

Considering the differences in electrospinning production conditions that produced pure PAN nanofiber with different properties, the best improvement ratio was obtained by the current method in terms of tensile strength and Young's modulus.

3.4. Impact on membrane pore sizes and permeation properties

In order to determine the impact of the PVDF addition on the membrane's matrix, porometry and permeability tests were performed. Porometry data of as-spun PAN and PVDF-c-PAN membranes are summarized in Table 5, including the mean flow pore size, bubble point pressure, bubble point flow rate, and pore diameter (μm), at 50% cumulative pore number.

Low values of bubble point pressure (representing the lowest pressure at which flow is sensed) and bubble point flow rate obtained in the blank indicate the presence of larger pores when compared to the other PVDF-c-PAN membranes. Fig. 7 illustrates that blank pore diameters at 50% are ≥ 1.36 with almost the twofold of PVDF-treated membranes values.

The mean flow pore size of the blank, A, and D were determined to be 1.511, 0.704, and 0.795 μm , respectively. Pores with larger diameter contain a greater proportion of the pore cross-sectional area than smaller diameter pores. Since lower pressure is required for flow to occur through larger pores than smaller pores, the mean pore diameter area may provide a better indication of which pores will actually be relevant in a filtration application.

Fig. 8 illustrates the histogram of pure water flux. As expected, the blank sample has the highest value

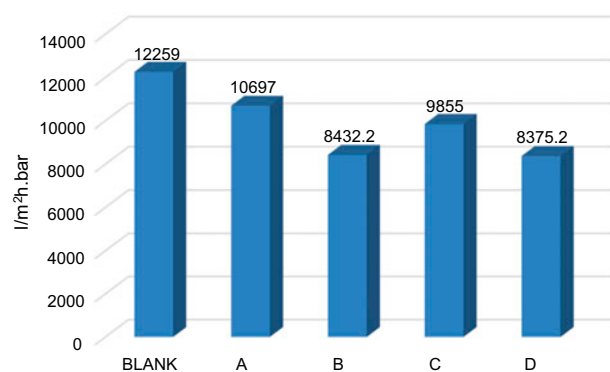


Fig. 8. Pure water flux for blank and PVDF-c-PAN nanofiber membranes.

which was $12,259 \text{ L m}^{-2} \text{ h}^{-1} \text{ atm}^{-1}$. The pure water flux reduction ratios for PAN-C-PVDF membranes A, B, C, and D were found to be 12.7, 31.2, 19.6, and 31.7%, respectively. This reduction was related to PVDF incorporation among nanofibers. By increasing PVDF concentration, PVDF intensity was also increased, as can be seen in SEM images (Fig. 3). PVDF made the resistance of membrane to increase against water flow, but at least membranes kept their superior permeability in a reasonable state, while increasing their mechanical properties.

4. Conclusion

In the study described above, we have explored the properties of electrospun PAN nanofibers, which were submerged in different PVDF concentrations. The effects of PVDF on the morphological and microstructural properties of the as-spun nanofibers were probed. Filtration test, SEM, DMA, and porometry were used to accomplish membrane characterizations. The results showed remarkable improvement in mechanical properties of the handled membranes without great trading off the membrane's flux performance.

This technique used in this study was compared to two different techniques that seek the improvement of the mechanical properties of the electrospun PAN nanofibers. In addition to its reasonable results, from application point of view, the current work technique is simple, practical, and time-cost saving.

References

- [1] B. Qiao, X. Ding, X. Hou, S. Wu, Study on the electrospun CNTs/Polyacrylonitrile-based nanofiber composites, *J. Nanomater.* 839462 (2011) 7.
- [2] L. Huang, J.T. Arena, S.S. Manickam, X. Jiang, B.G. Willis, J.R. McCutcheon, Improved mechanical properties and hydrophilicity of electrospun nanofiber membranes for filtration applications by dopamine modification, *J. Membr. Sci.* 460 (2014) 241–249.
- [3] S. Sundarajan, K.L. Tan, S.H. Lim, S. Ramakrishna, Electrospun nanofibers for air filtration applications, *Procedia Eng.* 75 (2014) 159–163.
- [4] S. Ramakrishna, R. Jose, P.S. Archana, A.S. Nair, R. Balamurugan, J. Venugopal, W.E. Teo, Science and engineering of electrospun nanofibers for advances in clean energy, water filtration, and regenerative medicine, *J. Mater. Sci.* 45 (2010) 6283–6312.
- [5] Available from: <<http://ieeexplore.ieee.org/stamp/stamp.jsp?tp=&arnumber=5424991>>.
- [6] A.G. MacDiarmid, W.E. Jones Jr., I.D. Norris, J. Gao, A.T. Johnson, N.J. Pinto, J. Hone, B. Han, F.K. Ko, H. Okuzaki, M. Llaguno, Electrostatically-generated nanofibers of electronic polymers, *Synth. Met.* 119 (2001) 27–30.
- [7] J. Chang, M. Dommer, C. Chang, L. Lin, Piezoelectric nanofibers for energy scavenging applications, *Nano Energy* 1 (2012) 356–371.
- [8] J.S. Lee, O.S. Kwon, S.J. Park, E.Y. Park, S.A. You, H. Yoon, J. Jang, Fabrication of ultrafine metal-oxide-decorated carbon nanofibers for DMMP sensor application, *ACS Nano* 5 (2011) 7992–8001.
- [9] J.M. Corres, Y.R. Garcia, F.J. Arregui, I.R. Matias, S. Member, Optical fiber humidity sensors using PVdF electrospun nanowebs, *Sensors J. IEEE* 11 (2010) 2383–2387.
- [10] W.J. Li, C.T. Laurencin, E.J. Caterson, R.S. Tuan, F.K. Ko, Electrospun nanofibrous structure: A novel scaffold for tissue engineering, *J. Biomed. Mater. Res.* 60 (2002) 613–621.
- [11] El-R. Kenawy, G. Bowlin, K. Mansfield, J. Layman, D. Simpson, E. Sanders, G. Wnek, Release of tetracycline hydrochloride from electrospun poly(ethylene-co-vinylacetate), poly(lactic acid), and a blend, *J. Controlled Release* 81 (2002) 57–64.
- [12] S. Lee, S.K. Obendorf, Use of electrospun nanofiber web for protective textile materials as barriers to liquid penetration, *Text. Res. J.* 77 (2007) 696–702.
- [13] J.A. Matthews, G.E. Wnek, D.G. Simpson, G.L. Bowlin, Electrospinning of collagen nanofibers, *Biomacromolecules* 3 (2002) 232–238.
- [14] C. Ren, PAN Nanofibers and Nanofiber Reinforced Composites, MSc Thesis, University of Nebraska, 2013.
- [15] L. Huang, S. Manickam, J. McCutcheon, Increasing strength of electrospun nanofiber membranes for water filtration using solvent vapor, *J. Membr. Sci.* 436 (2013) 213–220.
- [16] E.R. Cornelissen, Th. van den Boomgaard, H. Strathmann, Physicochemical aspects of polymer selection for ultrafiltration and micro-filtration membranes, *Colloids Surf. A* 138 (1998) 283–289.
- [17] N. Scharnagl, H. Buschatz, Polyacrylonitrile (PAN) membranes for ultra- and microfiltration, *Desalination* 139 (2001) 191–198.
- [18] A.K. Gupta, D.K. Paliwal, P. Bajaj, Melting behavior of acrylonitrile polymers, *J. Appl. Polym. Sci.* 70 (1998) 2703–2709.
- [19] Available from: <http://en.wikipedia.org/wiki/Polyacrylonitrile#cite_note-1> (n.d.).
- [20] H. Jiang, C. Wu, A. Zhang, P. Yang, Structural characteristics of polyacrylonitrile (PAN) fibers during oxidative stabilization, *Compos. Sci. Technol.* 29 (1987) 33–44.
- [21] Available from: <<http://www.dalau.com/pvdf.html>> (n.d.).
- [22] E.P.S. Tan, C.T. Lim, Mechanical characterization of nanofibers—A review, *Compos. Sci. Technol.* 66(9) (2006) 1102–1111.
- [23] X.F. Wang, K. Zhang, M.F. Zhu, B.J.S. Hsiao, B.J. Chu, Enhanced mechanical performance of self-bundled electrospun fiber yarns via post-treatments, *Macromol. Rapid Commun.* 29 (2008) 826–831.
- [24] M.R. Bilad, P. Westbroek, I.F.J. Vankelecom, Assessment and optimization of electrospun nanofiber-membranes in a membrane bioreactor (MBR), *J. Membr. Sci.* 380 (2011) 181–191.
- [25] S. Homaeigohar, M. Elbahri, Novel compaction resistant and ductile nanocomposite nanofibrous

- microfiltration membranes, *J. Colloid Interface Sci.* 372 (2012) 6–15.
- [26] K. Yoon, B. Hsiao, B. Chu, Formation of functional polyethersulfone electrospun membrane for water purification by mixed solvent and oxidation processes, *Polymer* 50 (2009) 2893–2899.
- [27] C. Zhang, Y. Li, W. Wang, N. Zhan, N. Xiao, S. Wang, Y. Li, Q. Yang, A novel two-nozzle electrospinning process for preparing microfiber reinforced pH-sensitive nano-membrane with enhanced mechanical property, *Eur. Polym. J.* 47 (2011) 2228–2233.
- [28] U. Stachewicz, F. Modaresifar, R.J. Bailey, T. Peijs, A.H. Barber, Manufacture of void-free electrospun polymer nanofiber composites with optimized mechanical properties, *ACS Appl. Mater. Interfaces* 4 (2012) 2577.
- [29] S. Kiani, S.M. Mousavi, N. Shahtahmassebi, E. Saljoughi, Preparation and characterization of polyphenylsulfone nanofibrous membranes for the potential use in liquid filtration, *Desalin. Water Treat.* (2015) 1–10.
- [30] R.O. Ritchie, The conflicts between strength and toughness, *Nat. Mater.* 10 (2011) 817–822.
- [31] D.K. Sharma, J. Shen, F. Li, Reinforcement of Nafion into polyacrylonitrile (PAN) to fabricate them into nanofiber mats by electrospinning: Characterization of enhanced mechanical and adsorption properties, *RSC Adv.* 4 (2014) 39110–39117.
- [32] Committee on High-Performance Structural Fibers for Advanced Polymer Matrix Composites, High-performance Structural Fibers for Advanced Polymer Matrix Composites, National Research Council, The National Academies Press, Washington, DC, 2005.
- [33] D. Papkov, Y. Zou, M.N. Andalib, A. Goponenko, S.Z.D. Cheng, Y.A. Dzenis, Simultaneously strong and tough ultrafine continuous nanofibers, *ACS Nano* 7 (2013) 3324–3331.
- [34] S. Huan, G. Liu, G. Han, W. Cheng, Z. Fu, Q. Wu, Q. Wang, Effect of experimental parameters on morphological, mechanical and hydrophobic properties of electrospun polystyrene fibers, *Materials* 8 (2015) 2718–2734.
- [35] X. Hou, X. Yang, L. Zhang, E. Waclawik, S. Wu, Stretching-induced crystallinity and orientation to improve the mechanical properties of electrospun PAN nanocomposites, *Mater. Des.* 31 (2009) 1726–1730.